Hayati, H., & Moss, R.E.S. (2017). "Strain Compatible Site Period, a New Perspective in Site Response Analysis." Soil Dynamics and Earthquake Engineering, 92C, pp. 551-560, DOI: 10.1016/j.soildyn.2016.10.010.

"Site response analysis considering strain compatible site period"

Hoss Hayati[a,*], Robb E.S. Moss[b]

[a] Geotechnical Engineer, SC Solutions, 1261 Oakmead Pkwy, Sunnyvale, CA 94085, USA
[b] Professor, Dept. of Civil Engineering, California Polytechnic State Univ., San Luis Obispo, CA 93407, USA

ARTICLE INFO

Keywords:
Site response
Single proxy
Strain compatible site period
VS30
Nonlinearity
Amplification factor
Site period shift

ABSTRACT

In practice it is common to estimate site effects using a single proxy, or single variable such as 30 m shear wave velocity (V_{S30}) or site period. Many studies have investigated merits of proposed proxies with contradicting recommendations. Yet, most studies indicate the single proxy approach is less than ideal, resulting in large uncertainty. To provide a better understanding of components that drive site response, we performed a parameterized study on 19 shallow soil profiles with V_S ranging from 150 m/s to 400 m/s. We propagated 74 input motions through each soil column using one-dimensional equivalent-linear method to produce 1406 site response analyses. The resulting amplification factors (the ratio of surface to base motion) were then analyzed statistically to identify trends. The mean amplification factor, averaged from 74 records, was used to isolate and quantify the effects of V_S on site response. Based on analysis of record-to-record trends, we identified two separate mechanisms through which nonlinearity affects site response including "damping increase" and "site period shift". The interaction of these two mechanisms makes amplification-shaking intensity models highly depth-dependent. The residual standard deviation of amplification factor based on depth-independent models was found to be up to three times larger than the corresponding standard deviation based on depth-specific models. We found strain compatible site period a promising site parameter that complements the predictive information obtained from V_S. Finally, a simplified procedure providing a five-point estimate of site transfer function is outlined. The proposed procedure can fill the gap in current practice for an intermediate solution between the numerically rigorous solution and the single proxy approach. Implementation of this procedure is demonstrated in an example.

1. Introduction

Two general approaches are used to estimate site effects on ground motion. A "site-specific" analysis is usually performed for sensitive buildings and large infrastructure like highway or railroad bridges, underground subway stations, lifelines, and dams. The site-specific analysis can be conducted using nonlinear or equivalent-linear methods to propagate shear waves from basement rock to the ground surface. Although three dimensional solutions are available for site response, in most cases a one dimensional (1-D) solution based on assumption of polarized upward/downward shear waves and infinite horizontal layers is practiced. Implementation of site-specific analysis requires resources that may not be readily available for small to medium size projects or in conceptual/bid phase of large projects. Alternatively, generic site factors are used for final design of typical buildings, a wide range of small infrastructure, and in conceptual phase design of large infrastructure. Developing site factors has been done by compiling ground motion data recorded at soil and rock sites during past earthquakes and examining dependence of amplification factor on certain site parameter, also known as site proxy, using multivariable regression techniques (e.g., [1,3,5,6,13,16,26].

The most commonly used site proxies include descriptive geotechnical or geological classification, shear wave velocity (V_S) averaged in top 30 m (V_{S30}), or site period (T_N). Borcherdt [5] analyzed site response data from 1989 Loma Prieta earthquake and suggested a linear relationship between amplification factor and V_{S30} in natural log scale at short and mid periods for two ranges of peak ground acceleration (PGA) of $< 0.2g$ and $> 0.2g$. Accordingly, a site classification was proposed based on V_{S30} to estimate site factors which were later adopted by the UBC1997 Code [27] and NEHRP Provisions (2009) [17]. Probabilistic seismic hazard analysis (PSHA) practice has gradually evolved to adopt the V_{S30}-based approach by incorporating V_{S30} and various depth-related terms, (e. g. depth to V_S =1000 m/s) in ground motion prediction equations (GMPE) including Next Generation of Attenuation (NGA) models (eg. [2,7,8,12].

The single proxy approach is simple to use but omits several key

* Corresponding author.
E-mail address: hhayati@scsolutions.com (H. Hayati).

components of site response which leads to large uncertainty of the results. For example, site factors developed from 1989 Loma Prieta earthquake data by Borcherdt [5] have an standard error of regression of 0.5–0.65 in natural log scale. Choi and Stewart [13] developed amplification factors as a continuous function of V_{S30} and shaking intensity with a regression error ranged from 0.45 to 0.69 in natural log scale. Estimation of amplification factor with an error of such magnitude makes the applicability of the developed transfer functions limited.

There have been numerous studies focusing on merits of various site proxies with contradicting recommendations. Rodriguez et al. [20] used site response data from 1989 Loma Prieta and 1994 Northridge earthquakes to examine the accuracy of various site classification systems. They compared the V_{S30}-based classification and a site period-based classification and found the two systems provide similar accuracy in prediction of site response. Stewart et al. [23] used 1828 records from 154 shallow crustal earthquakes and found that a detailed-surface geology classification provides a more accurate prediction of site amplification than either the V_{S30}-based or a site period-based classification system for soil sites. Abrahamson [2] favored V_{S30} as a less subjective site parameter to be used in GMPE for deep soil sites common in California and suggested other site parameters can be added to GMPEs. Site period has been found an adequate site parameter by a handful of scholars (e.g. [29,10,19]). Zhao [30] used 3018 KiK-net downhole array record pairs (surface and borehole) from 95 earthquakes in Japan and developed a model for surface/borehole amplification factors. Based on this study, site period was found a better site proxy with lower standard deviation of inter-site residuals of amplification ratios compared to V_{S30} for spectral periods >0.6 s. McVerry [19] analyzed the strong ground motion data that was used in developing New Zealand GMPEs and found site period is a more adequate predictor of site effects than V_{S30}, in particular, for deep/stiff sites. Castellaro [9] ran one dimensional equivalent-linear site response simulations for a suite of 585 soil profiles and two simple records including a Ricker wavelet with frequency of 1 Hz and 0.5 Hz and showed a matrix consisting of shear wave velocity of shallower softer layer, site period, and site impedance ratio predicts amplification factor better than V_{S30}.

Although a large number of studies suggested the inadequacy of the single proxy approach in general, and V_{S30} as the single site proxy in particular, no consensus has emerged for an alternative approach. The inconclusive research may be attributed to complexity of site response problem which is inherently unresolvable to a single predictor. This paper presents a parametric study of multiple components that are omitted in single proxy approach. The methodology includes performing 1-D site response analysis by propagating 74 ground motions through a suite of hypothetical soil profiles. The resulting suite of amplification factors is analyzed statistically to identify trends. This study attempts to provide some perspective on "which single proxy? " through a better understanding of the contribution of shear wave velocity, site period, and site period shift due to nonlinear soil behavior.

2. Methodology

The general methodology used here is similar to the approach used by [4], [28], and Castellaro [9]. In particular, this study was performed to build upon findings of [4]. The set of soil profiles used in this study covers a broader condition than the set used in [4]. This study includes 19 soil profiles, with V_S ranging from 150 m/s to 400 m/s and the depth to bedrock ranging from 10 m to 75 m. Two soil types, a generic sand and a generic clay (with plasticity index of 40–80) were used. The shear stiffness degradation and damping versus shear strain models [14,21,22,24] for these materials are plotted in Fig. 1. A summary of soil profiles along with the material type, V_S, and site periods are presented in the Table 1. Bedrock was assumed to have a V_S of 760 m/s to match the boundary between NEHRP B and C classes.

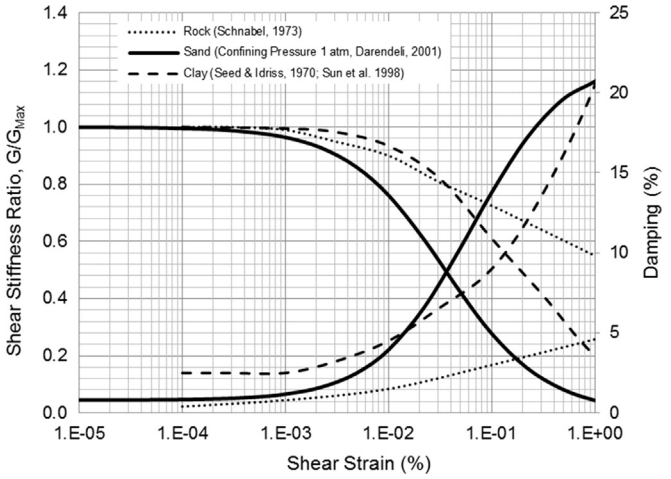

Fig. 1. Stiffness degradation and damping curves for materials used in this study.

Table 1
Hypothetical soil profiles used in this study.

Profile	Soil Type	Depth to bedrock (m)	V_S (m/s)	T_N (s)
S–75–400	Sand	75	400	0.75
S–75–316	Sand	75	316	0.95
S–75–200	Sand	75	200	1.50
S–50–400	Sand	50	400	0.50
S–50–316	Sand	50	316	0.63
S–50–200	Sand	50	200	1.00
S–25–400	Sand	25	400	0.25
S–25–316	Sand	25	316	0.32
S–25–200	Sand	25	200	0.50
C–75–400	Clay	75	400	0.75
C–75–316	Clay	75	316	0.95
C–75–200	Clay	75	200	1.50
C–50–400	Clay	50	400	0.50
C–50–316	Clay	50	316	0.63
C–50–200	Clay	50	200	1.00
C–25–400	Clay	25	400	0.25
C–25–316	Clay	25	316	0.32
C–25–200	Clay	25	200	0.50
S–10–150	Sand	10	150	0.27

A total number of 74 records from 27 earthquakes after [4] were run through each soil profile. Most of the ground motions were recorded at rock sites with average V_S of 760 m/s. The recording at the bedrock level is not equal to the recording at a nearby rock outcrop due to reflections and weathering of surficial rock. Following [4], we did not perform deconvolution for two reasons, (1) the main objective of this study is not to provide the best estimate of amplification factor but to investigate parameters and procedures that will lead to better estimate of amplification factor, (2) deconvolution is expected to impact site response at very short period range. Such period range is not usually of interest for infrastructure projects like bridges and tall buildings.

A list of records used in this study and the corresponding spectral accelerations are provided in the electronic supplement. The earthquake magnitudes range from M5.0 to M7.4 with a median value of M6.7, and *PGA* ranges from 0.01 g to 1.5 g, with median and geometric mean values 0.11 g. The ground motion database used in this study is available at Pacific Earthquake Engineering Research Center website (www.peer. Berkeley.edu; accessed November 2010).

We performed equivalent-linear 1-D site response analysis on each soil profile using SHAKE2000 [18]. The appropriate shear strain range for application of equivalent linear method is investigated in several past studies. Bolisetti et al. [11] conclude that the equivalent linear response is inappropriate when shear strain is greater than 1%. Kaklamnous et al. [15] recommended nonlinear method be used for

Table 2
Standard deviation of amplification facto,$\sigma_{Ln(AF)}$.

Profile	Depth-independent model					Depth-specific model				
	Peak	0.1 s	0.6 s	1.0 s	3.0 s	Peak	0.1 s	0.6 s	1.0 s	3.0 s
S–75–400	0.062	0.254	0.222	0.212	0.087	0.056	0.189	0.088	0.115	0.073
S–50–400						0.062	0.162	0.123	0.089	0.052
S–25–400						0.060	0.136	0.086	0.083	0.034
S–75–316	0.083	0.279	0.263	0.250	0.140	0.079	0.238	0.095	0.140	0.111
S–50–316						0.081	0.204	0.115	0.145	0.082
S–25–316						0.074	0.155	0.139	0.108	0.051
S–75–200	0.123	0.427	0.364	0.348	0.240	0.104	0.341	0.231	0.131	0.126
S–50–200						0.097	0.285	0.119	0.169	0.139
S–25–200						0.116	0.220	0.173	0.188	0.099
C–75–400	0.051	0.186	0.160	0.181	0.061	0.044	0.167	0.069	0.068	0.055
C–50–400						0.055	0.114	0.073	0.068	0.047
C–25–400						0.054	0.100	0.062	0.049	0.026
C–75–316	0.070	0.221	0.210	0.230	0.100	0.074	0.217	0.095	0.096	0.084
C–50–316						0.071	0.188	0.100	0.081	0.067
C–25–316						0.062	0.112	0.089	0.084	0.039
C–75–200	0.110	0.355	0.335	0.268	0.206	0.104	0.290	0.120	0.112	0.121
C–50–200						0.108	0.236	0.123	0.116	0.123
C–25–200						0.115	0.177	0.144	0.105	0.076
S–10–150	Not Calculated					0.119	0.241	0.166	0.154	0.069

shear strain greater than 0.4% at short periods, and suggested both equivalent-linear and non-linear methods provide similar results at long period. For the purpose of this study, for each profile, records that induce shear strain values of greater than 0.8% were excluded from our analysis. The number of ground motion records that were excluded ranged from 0 to 8 of the 74 records for different profiles. We also considered setting a lower threshold of 0.5% for shear strain to comply with findings of Kaklamnous et al. [15] This lower threshold would have resulted in exclusion of 0–3 more records from our analysis for some of the softer profiles. We proceeded with a threshold shear strain of 0.8% as it would not affect our key findings.

3. Limitations

We recognize that site response is a complex problem and several contributing components including 3-D effects, topography effects, spatial variability of soil properties and ground motion, incidence angles, primary wave effects, and integrity of bedrock, among others, are excluded from the scope of this study. The idealized conditions of a uniform soil layer over bedrock limits the applicability of our findings. However, this approach reduces the number of contributing components on site response. Such idealization was necessary for tracking the impact of individual components like V_S, site period, and site period shift which could be masked when using more complicated soil profiles based on empirical data. Applicability of our findings is limited to low and medium strain range where use of equivalent-linear method is justified. The impact of nonlinear soil behavior on site response is expected to be more pronounced in very short period range. This period range is of less interest for major infrastructure for which a site-specific site response analysis is sought. Finally, our results do not apply when ground failure including liquefaction, cyclic softening, and excessive seismic deformations take place.

4. Results

It is helpful to define several terms that we use frequently from this point forward. Site period, T_N, is the period at which soil column would resonate with harmonic loading and can be computed as: $T_N = 4\,H/V_S$, where H is depth to bedrock. Strain compatible shear wave velocity, V_S^*, is computed from strain compatible shear stiffness, G^*, through $G^* = \rho.\,(V_S^*)^2$ where ρ is density. G^* is a function of shear strain and is determined from the stiffness degradation curve. Strain compatible site period, T_N^*, is computed as $T_N^* = 4\,H/V_S^*$. The analysis results are first presented for the mean response for each profile averaged from 74 records, followed by the results from individual records.

4.1. Dependence of amplification factor on V_S

Amplification factor for 5% damped response spectral acceleration, AF, was computed for each ground motion. We then averaged the amplification factor from the 74 records at any given period, AF_m. Plotted in Fig. 2(a), b, and c are AF_m for generic clay with V_S =400 m/s, 316 m/s, and 200 m/s, respectively. Similar graphs for generic sand are provided in the electronic supplement. Peak amplification factor [maximum amplification factor across the period range] is denoted by AF_{Pm}. Note that AF_{pm} increases as V_S reduces but remains approximately constant as depth to bedrock increases. Also, note the period at which AF_{pm} occurs increases as depth to bedrock increases. This period for each soil profile is the strain compatible site period (T_N^*). AF_{Pm}, is plotted versus V_S in Fig. 3 with each data point representing peak amplification factor averaged from 74 records for one soil profile. We found a strong linear correlation between AF_{Pm} and V_S with coefficients of determination R^2 greater than 0.96. AF_{Pm} can be estimated from the following equations where V_S is in m/s:

$$\text{Generic Sand}\ \ \mathrm{Ln}(AF_{Pm}) = -0.40Ln(V_S) + 3.07 \quad (1)$$

$$\text{Generic Clay}\ \ Ln(AF_{Pm}) = -0.54Ln(V_S) + 3.81 \quad (2)$$

Since AF_{Pm} is averaged from 74 records it has minimal representation of "shaking intensity" and "record-to-record" variability. Also, it was shown AF_{Pm} is independent from depth to bedrock. This would make AF_{Pm} a good parameter to use for tracking and quantifying the impact of V_S on site response. Therefore, Eqs. (1) and (2) provide a useful tool to characterize the isolated impact of V_S on amplification factor.

4.2. Amplification factor vs shaking intensity

In this section we investigate the relationship between amplification factor and shaking intensity, also known as nonlinearity model. We examined various shaking intensity parameters, and similar to Bazzurro and Cornell [4], found amplification at any period is best correlated with response spectral acceleration of bedrock at corresponding period, S_a. Peak amplification factor across the period range for an individual record, AF_P was found best correlated with spectral

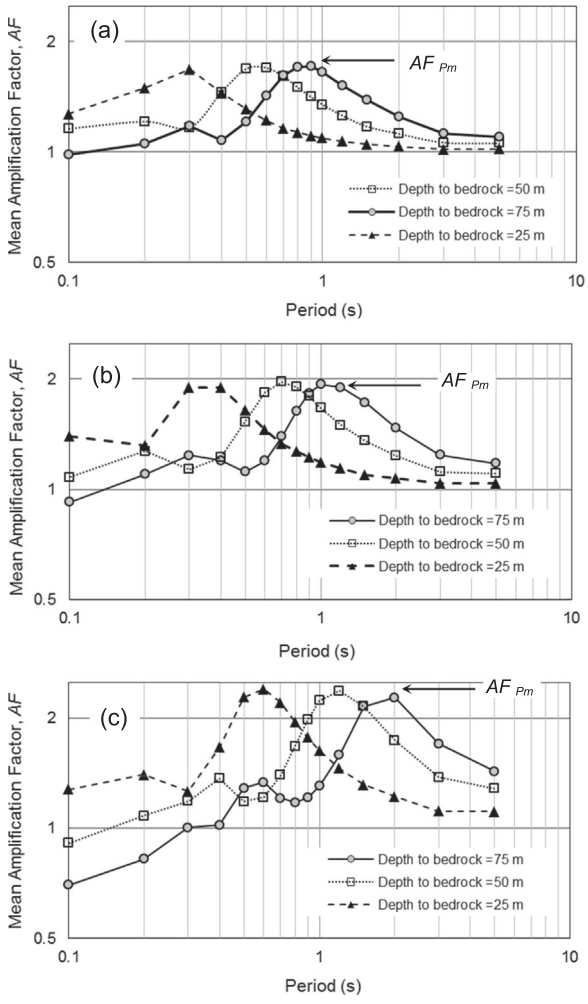

Fig. 2. Amplification transfer functions averaged from 74 records for gneric clay (a) V_S =400 m/s, (b) V_S =316 m/s, (c) V_S =200 m/s.

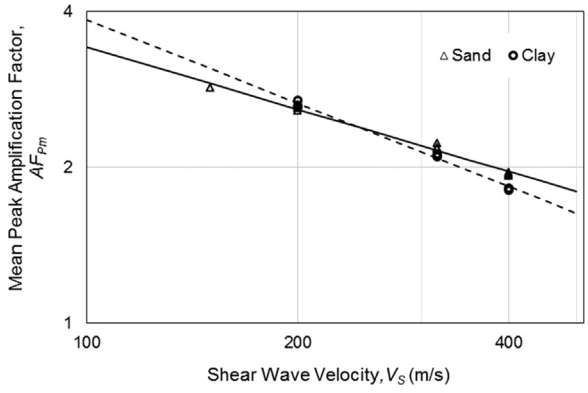

Fig. 3. Peak amplification factors averaged from 74 records versus shear wave velocity.

acceleration of bedrock at site period, S_a^F. Plotted in Fig. 4(a) to (d) are amplification factors at periods of 0.5 s, 1.0 s and 1.5 s, and peak amplification, AF_P, versus spectral acceleration of input motion for generic sand with V_S=316 m/s, depth to bedrock of 50 m and site period of 0.63 s (=4×50 m/316 m/s). Each data point shown in Fig. 4 represents an individual record. The following distinct trends for nonlinearity were identified:

- $AF_{0.5}$ shows a strong negative correlation with S_a,
- $AF_{1.0}$ first increases with S_a and then drops as S_a increases,
- $AF_{1.5}$ shows a mild positive correlation with S_a, and
- AF_P shows a mild negative correlation with S_a.

To explain these trends, two major mechanisms through which nonlinearity operates, should be recognized:

A. Damping increase which de-amplifies the motion as acceleration increases,
B. Stiffness decrease and migration of site period which may amplify or de-amplify the motion due to resonance effects.

For $AF_{0.5}$, the designated period of 0.5 s is smaller than the small strain site period, T_N, of 0.63 s. As S_a increases, strain compatible site period, T_N^*, migrates away from designated period of 0.5 s and resonance effects diminish resulting in amplification reduction. Concurrently, as S_a and shear strain increase, higher damping tends to de-amplify the motion. For $AF_{0.5}$ mechanisms A and B act in parallel leading to strong negative correlation between amplification and S_a. For amplification at period of 1.0 s and within the range of approximately S_a < 0.2 g, as S_a increases, amplification increases. In this range, strain compatible site period, T_N^*, falls between 0.63 s and 1.0 s; as S_a increases, T_N^* shifts towards resonance period of 1.0 s which results in amplification increase. In this range mechanism A and B operate in opposite, but, mechanism B controls. For S_a > 0.2 g, T_N^* is greater than resonance period of 1.0. In this range, as S_a increases, site period shifts away from designated period of 1.0 s, combined with increased damping effects, results in sharp reduction of amplification. For $AF_{1.5}$, T_N^* for all records is less than the designated period of 1.5 s. Therefore, as S_a and T_N^* increase, amplification mildly increase due to resonance indicating mechanism B is controlling. Finally peak amplification, AF_P always occurs at T_N^* and migration of site period is not relevant. For AF_P nonlinearity is controlled only by mechanism A. As a result, amplification mildly reduces as S_a increases. The widely accepted notion, incorporated in building codes, suggests amplification factor reduces with shaking intensity due to nonlinear soil behavior. Different trends described above indicate the impact of "shaking intensity" is complex; amplification may increase with shaking intensity when site period shifts toward period of interest.

4.3. Depth-dependency of amplification-shaking intensity (AF-S$_a$) Models

Plotted in Fig. 5(a), (b) and (c) are amplification factor, *AF*, at periods of 0.1 s, 0.6 s, and 1.0 s, respectively, versus bedrock spectral acceleration, S_a, at corresponding periods for sand profiles with V_S =200 m/s and depths to bedrock of 25 m, 50 m, and 75 m. Peak amplification factor, AF_P, is plotted versus bedrock spectral acceleration at site fundamental period, S_a^F, in Fig. 5(d). Note that while data point clusters corresponding to different depths are visually separated in Fig. 5(a), (b) and (c), data points of different depths for peak amplification are intermixed in Fig. 5(d). For each soil profile, the best fitted quadratic or bi-linear function (in log scale) is also plotted following Bazzurro and Cornell (2004). Fitted curves for depth to bedrock of 25 m, 50 m and 75 m are distinct in Fig. 5(a), (b) and (c) suggesting amplification versus shaking intensity (*AF-S$_a$*) models are depth-dependent at periods of 0.1 s, 0.6 s and 1.0 s. Note; however, a depth-independent model seems appropriate for peak amplification.

To statistically test this observation, we computed the residual standard deviation of amplification factor, $\sigma_{Ln(AF)}$, after accounting for its dependence on S_a. $\sigma_{Ln(AF)}$ represents the random "record-to-record" variability of amplification factor and can be computed using the following equation:

$$\sigma_{Ln(AF)}=\sqrt{1-R^2}\,\sigma'_{Ln(AF)} \quad (3)$$

where $\sigma'_{Ln(AF)}$ is the standard deviation of amplification factor calculated from 74 records for each profile at designated period and, R^2 is

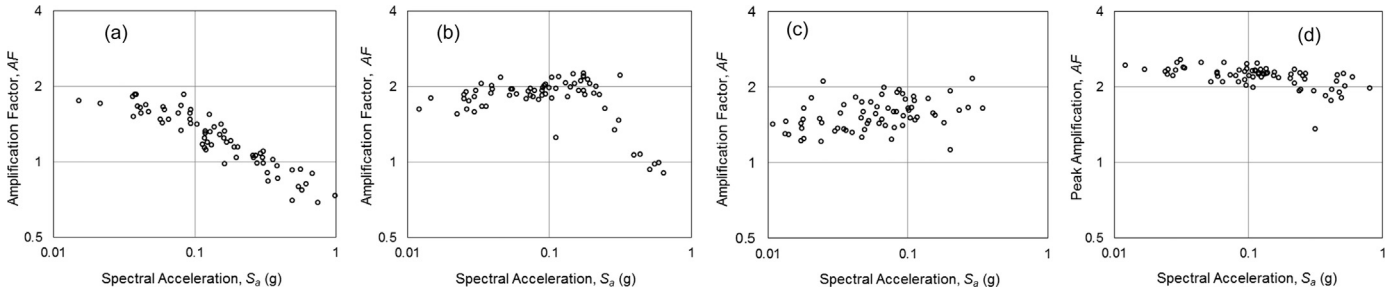

Fig. 4. Amplification versus spectral acceleration for generic sand, depth to bedrock 50 m, V_S=316 m/s, (a) 0.5 s, (b) 1.0 s, (c) 1.5 s, (d) Peak.

the coefficient of determination computed for *AF* versus S_a. Presented in Table 2 are $\sigma_{Ln(AF)}$ values based on using two sets of R^2 values obtained from depth-specific and depth-independent *AF*-S_a models. Note the following trends:

- $\sigma_{Ln(AF)}$ based on depth-independent model is larger than the corresponding value computed using the depth-specific models. For example, for sand with *Vs* =200 m/s, $\sigma_{Ln(AF)}$ for depth-independent model is 1.5–3 times larger than $\sigma_{Ln(AF)}$ based on depth-specific models. Depth-independent models generate a large uncertainty which is epistemic in nature, that is, can be removed if model takes into account the depth effects.
- $\sigma_{Ln(AF)}$ for peak amplification is similar using either models ranging from 0.04 to 0.12.
- Similar to findings of Bazzurro and Cornell (2004), $\sigma_{Ln(AF)}$ at long period is relatively small ranging from 0.03 to 0.13.
- $\sigma_{Ln(AF)}$ ranges from 0.06 to 0.34 at short and mid periods which generally agrees with $\sigma_{Ln(AF)}$ range of less than 0.3 reported by Bazzurro and Cornell [4].
- Bazzurro and Cornell' [4] study was performed on two specific sites. These results verify and extend their findings to a broader range of soil and site conditions.

4.4. Strain compatible site period, a prospective parameter

It was shown that site period shift in nonlinear strain range can have a critical impact on site response. None of the currently proposed site or motion parameters in the scope of single proxy approach properly captures this effect. In our search, we found strain compatible site period, T_N^*, a promising parameter that holds key predictive information including "shaking intensity", "site period" and "site period shift".

SHAKE2000 computes strain compatible shear wave velocity, V_S^*, for each sub-layer from calculated shear strain at the end of iteration in equivalent-linear method and using G/G_{max} curves. V_S^* is then averaged from sublayers to compute V_S^* and T_N^* [=4 H/ V_S^*] for soil column. For the purpose of this study, T_N^*, was provided for each record by SHAKE2000. Plotted in Fig. 6(a) through (d) are amplification factors at periods of 0.1 s, 0.6 s, 1.0 s and 3.0 s versus T_N^*. Each plot includes data from 19 profiles excited by 74 motions producing 1406 data points. Also are plotted mean amplification factors for each soil profile averaged from 74 records, AF_m, using red solid circle marker. These plots put various components that contribute in site response in a holistic prospective. Three major components drive site response including T_N^*, V_S, and damping. The following trends can be identified based on these components:

4.5. V_S -based trend

A visual examination of data clusters of different profiles at 0.1 s, 0.6 s, and 1.0 s shows that for a similar T_N^* data points corresponding to profiles with lower V_S tend to fall above data clusters with higher V_S. This observation is another expression of the trend identified for amplification factor as a function of V_S in Eqs. (1) and (2).

4.6. T_N^*-based Trend

Note that in each plot amplification factor peaks when site period matches period of interest. Amplification at 0.1 s steadily decreases as T_N^* shifts away from 0.1 s. Amplification at 0.6 s shows two peaks at 0.6 s and 1.8 s corresponding to the first and the second fundamental site period. Amplification at 1.0 s peaks at 1.0 s. Amplification at 3.0 s steadily increases as T_N^* approaches 3.0 s. These trends can be explained by *resonance*.

We used the mean amplification factors, AF_m, each representing the average site response from 74 records for a single site to generate amplification factor versus T_N^* trend curves. Before generating trend curve, AF_m values were normalized to remove V_S effects by applying a correction factor based on Eqs. (1) and (2). For example, AF_m at 0.6 s for profile S-75–400 (V_s=400 m/s) is 1.20. To compute amplification factor for V_s=300 m/s, we used Eq. (2) (generic sand) which provides AF_m equal to 1.96 and 2.20 for V_s=400 m/s and V_s=300 m/s, respectively. The conversion factor (in natural log scale) is calculated as *Ln* (2.20) −*Ln* (1.96) =0.12. The corrected amplification factor for V_s =300 m/s is then computed as *Exp*[*Ln*(1.2)+0.12] =1.35. Using similar method, three sets of AF_m values for V_S =200 m/s, 300 m/s, and 400 m/s were generated. A trend curve was then *manually* drawn for each AF_m set. Amplification factors at 3.0 s do not show a clear dependency on V_S, therefore, a single curve was plotted without adjusting for V_S. However, our relatively shallow soil profiles may

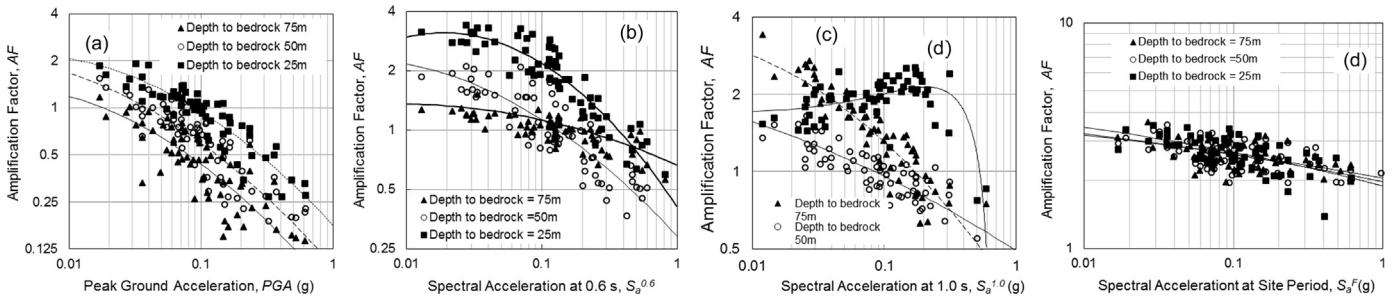

Fig. 5. Amplification factor versus spectral acceleration for generic sand with V_S =200 m/s at (a) 0.1 s, (b) 0.6 s, (c) 1.0 s, (d) peak amplification factor.

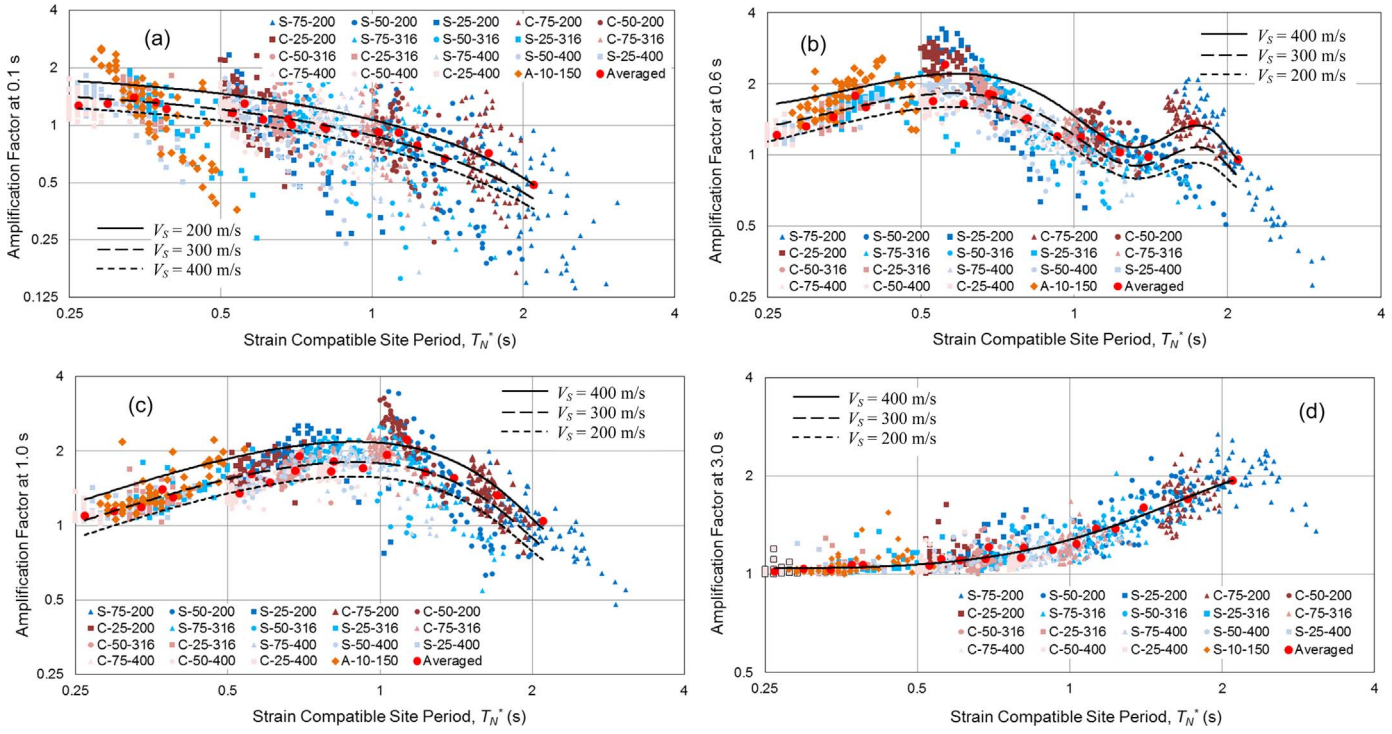

Fig. 6. Amplification factor versus strain compatible site period at (a) 0.1 s, (b) 0.6 s, (c) 1.0 s, (d) 3.0 s.

not allow seeing the dependency of long-period amplification on V_S. It is likely that amplification at long period would show dependency on V_S in deep sites where depth is large compared to wave length.

Amplification factors from individual records also follow similar trend lines set by mean amplification factors; for each soil profile, *AF* increase as T_N^* approaches period of interest, and decrease as T_N^* shifts away from period of interest. This indicates T_N^* not only holds predictive information about average response of different soil profiles but also record-to-record variation of response for a given soil profile.

4.7. Damping-based trend

In each plot a damping-controlled zone is identified in which data points show a larger scatter around T_N*-based trend line set by mean amplification factors. This zone includes the range of T_N^* > period of interest in each plot; that is, 0.1 s < T_N^* in Fig. 6(a), 0.6 s < T_N^* in Fig. 6(b), and 1.0 s < T_N^* in Fig. 6(c). In damping control zone, *AF* reduces as T_N^* increases following a steeper slope than the slope of the T_N*-based curve set by mean amplification factors. In damping-controlled zone as T_N* shifts away from resonance period, damping increase and site period shift [nonlinearity mechanisms A and B discussed in previous section] concurrently de-amplify the motion resulting in a sharp reduction of amplification factor.

We used a method that is schematically illustrated in Fig. 7 to quantify damping effects. According to this method, when T_N^* < period of interest, amplification factor can be directly read from T_N*-based trend line. When T_N^* > period of interest; first, the mean amplification factor for soil profile, AF_m, is computed by the T_N*-based curve, then, amplification factor for a specific record is corrected for damping using amplification-shaking intensity (*AF*-S_a) relationships. We plotted *AF* versus S_a at periods of 0.1 s, 0.6 s, and 1.0 s period (similar to Fig. 5). The best fitted model is quadratic [4] and can alternatively be modeled as bilinear with two distinct slopes b_1 for $S_a < S_{am}$, and b_2 for $S_a > S_{am}$ where S_{am} is the spectral acceleration averaged from 74 records. For records included in our dataset S_{am} is $0.1g$, $0.12g$, and $0.09g$, for periods of 0.0 s (*PGA*), 0.6 s, and 1.0 s, respectively. We assumed the mean amplification factor, AF_m, obtained from T_N*-based curve corresponds to S_{am} of approximately $0.1g$. For S_a greater or smaller than S_{am}, *AF* should be corrected to account for damping using the following equations:

$$Ln(AF_{Sa}) = Ln(AF_m) + \Delta\, Ln(AF_{Sa}) \quad (4)$$

where AF_{Sa} is the amplification factor corresponding to specific record with shaking intensity of S_a. Mean amplification, AF_m, is computed

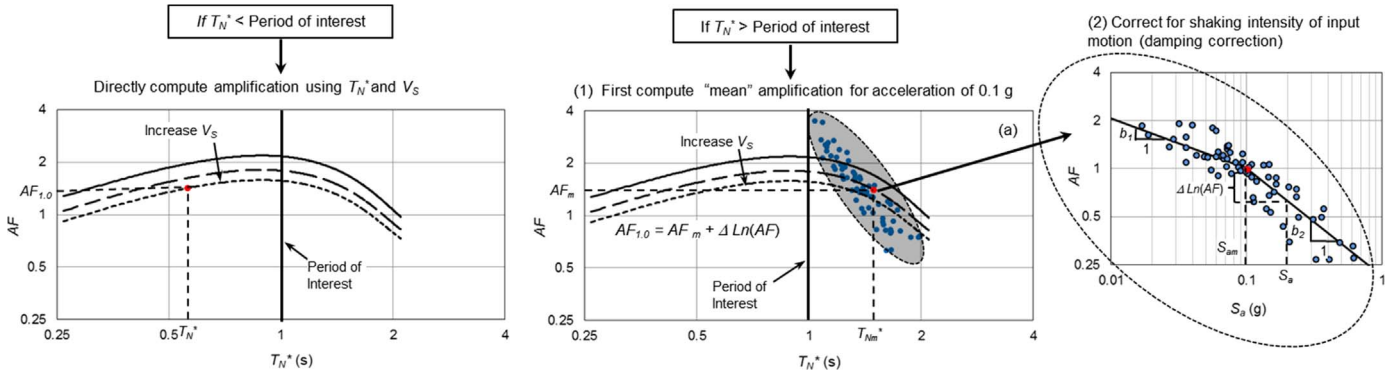

Fig. 7. Schematic illustration of simplified procedure to correct amplification factor for damping effects.

Table 3
Calculated b_1 and b_2 for soil profiles.

Period	Peak	0.1 s		0.6 s		1.0 s	
Profile	b_1=b_2	b_1	b_2	b_1	b_2	b_1	b_2
A–75–400	0[1]	−0.113	−0.579	−0.083	−0.238	NC[2]	−0.315
A–75–316	−0.048	−0.213	−0.613	NC[2]	NC[2]	NC[2]	−0.398
A–75–200	−0.125	−0.380	−0.725	−0.302	−0.553	−0.222	−0.218
A–50–400	0[1]	−0.156	−0.555	−0.030	−0.251	NC[2]	NC[2]
A–50–316	−0.066	−0.111	−0.666	−0.138	−0.402	NC[2]	NC[2]
A–50–200	−0.089	−0.370	−0.603	NC[2]	NC[2]	−0.317	−0.342
A–25–400	0[1]	−0.156	−0.423	NC[2]	NC[2]	NC[2]	NC[2]
A–25–316	−0.057	−0.150	−0.557	NC[2]	NC[2]	NC[2]	NC[2]
A–25–200	−0.130	−0.292	−0.631	−0.208	−0.686	NC[2]	NC[2]
B–75–400	0[1]	−0.032	−0.259	0.000	−0.090	NC[2]	NC[2]
B–75–316	−0.014	−0.047	−0.259	NC[2]	NC[2]	NC[2]	−0.073
B–75–200	−0.057	−0.180	−0.403	−0.140	−0.138	−0.097	−0.197
B–50–400	0[1]	−0.101	−0.203	−0.050	0.000	NC[2]	NC[2]
B–50–316	−0.026	−0.047	−0.299	−0.054	−0.112	NC[2]	NC[2]
B–50–200	−0.067	−0.137	−0.394	NC[2]	NC[2]	−0.075	−0.227
B–25–400	0[1]	−0.047	−0.069	NC[2]	NC[2]	NC[2]	NC[2]
B–25–316	−0.032	−0.094	−0.228	NC[2]	NC[2]	NC[2]	NC[2]
B–25–200	−0.056	−0.167	−0.386	−0.106	−0.098	NC[2]	NC[2]

NC[2] Not calculated
[3]Not sufficient data to compute b values
[1] For AFP, and for VS=400 m/s, AF-Sa relationships show a very weak correlation resulting in approximately b1=b2 =0.

from T_N^*-based curve for S_{am} =0.1g in Fig. 6, and:

$$\Delta\, Ln(AF_{Sa}) = b.\,[Ln(S_a) - Ln(S_{am})] \quad (5)$$

where

$$b = b_1 \text{ for } S_a < S_{am}, \text{ and } b = b_2 \text{ for } S_a > S_{am} \quad (6)$$

b_1 and b_2 were computed for peak amplification and amplification factors at periods of 0.1 s, 0.6 s, and 1.0 s for soil profiles in this study and listed in Table 3. We only included profiles with data points that fell on right side of the peak amplification in Fig. 6 to ensure they are in damping-controlled zone. Values of b_1 and b_2 should be treated with discretion as they are developed based on a limited data.

4.8. Simplified procedure

There is a need in current state of practice for an intermediate solution between rigorous site response analysis based on nonlinear or equivalent-linear solutions in one end and the single proxy approach used to estimate generic site factors on the other end. An intermediate approach would be very useful to provide a preliminary estimate of seismic demands in conceptual/bid design of large infrastructures as well as final design of small critical structures which exclusively rely on NEHRP site factors to account for site response. In absence of an intermediate solution practitioners may apply arbitrary factors of safety on seismic demand estimated from GMPEs. For example, 84 percentile spectral accelerations may be used (mean spectral acceleration plus one standard deviation of approximately 0.35 in natural log scale). Such factor of safety implies a uniform amplification factor across the period range. This approximation does not maintain the rigor of PSHA practice so that consistency is lost between the PSHA and the site response. Our findings presented in this study were used to develop a simplified procedure including the following steps:

Step 1: Determine site parameters including V_S, depth to bedrock (H), and site period, T_N (=4 H/V_S).

Step 2: Determine motion parameters including spectral acceleration of ground motion at 0.0 s (*PGA*), 0.6 s, and 1.0 s

Step 3: **Estimate strain compatible site period, T_N^***. It was mentioned that SHAKE2000 provided T_N^* for each profile and each record. For profiles included in our dataset, we found V_S^* and spectral acceleration at site period, S_a^F, are strongly correlated with coefficients of determination R^2 mostly above 0.8. Plotted in Fig. 8 are V_S^* versus S_a^F for generic sand and clay and V_S =400 m/s and 200 m/s. Use interpolation to estimate V_S^* for other values of depth to bedrock and V_S. Note two sets of strain compatible site period should be computed:

- Use Fig. 8 and S_a =0.1g to estimate mean strain compatible site period, T_{Nm}^*
- Use Fig. 8 and S_a =S_a^F (spectral acceleration at site period for ground motion of interest) to compute strain compatible site period, T_N^*

Step 4: Compute amplification factor at periods of 0.1 s, 0.6 s, 1.0 s and 3.0 s Use Fig. 6 to first estimate mean amplification factor. Use method shown in Fig. 7 to correct for damping. If T_N^* < period of interest, no damping correction is required.

Step 5: Compute peak amplification factor. Maximum amplification factor across period range, AF_P, which occurs at site period, T_N^*, can be estimated in two steps: 1) use Eqs. (1) and (2) to predict the mean value of peak amplification factor (averaged from 74 records), 2) use Table 3 to find b_1 or b_2, use Eq. (4) through 6 to correct for damping effects. This procedure is schematically shown in Fig. 9. Note the input spectral acceleration in Fig. 9(b) is spectral acceleration of bedrock at site period.

This procedure provides amplification factors at periods of 0.1 s, 0.6 s, 1.0 s, 3.0 s, and also peak amplification factor to create a five-point estimate of transfer function. Interpolation can be used to compute amplification at intermediate periods. The proposed procedure can be conveniently implemented in spreadsheet. The application of proposed procedure would be subject to limitations of the methodology and range of soil conditions used in this study.

4.9. Example

Strong amplification of ground motion due to underlying thick clay deposits was widely observed in city of Oakland during the 1989 Loma Prieta earthquake [25]. The proposed procedure was tested for the case of Oakland 2-story building site [25]. We used the outcrop rock motion recorded at the nearby Yerba Buena Island station (90 deg) as input motion. The 5% damped response spectra of the outcrop motion and

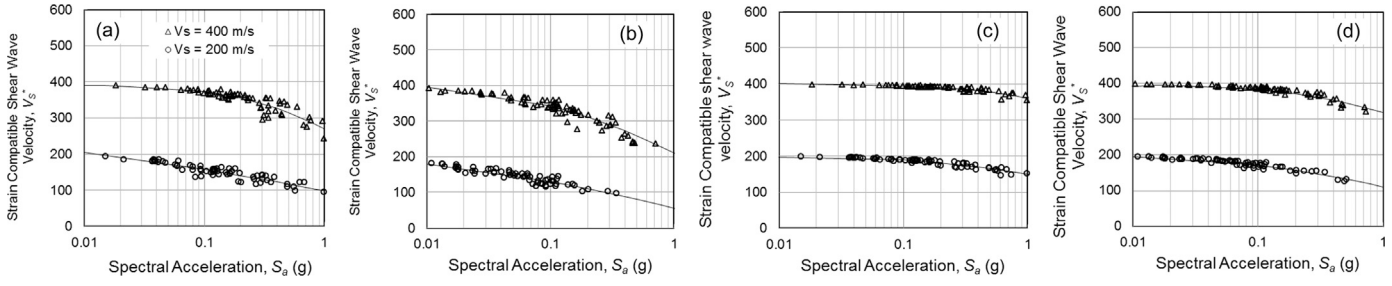

Fig. 8. Strain compatible shear wave velocity versus spectral acceleration, (a) Sand, depth to bedrock 25 m, (b) Sand, depth to bedrock 75 m, (c) Clay, depth to bedrock 25 m, (d) Clay, depth to bedrock 75 m.

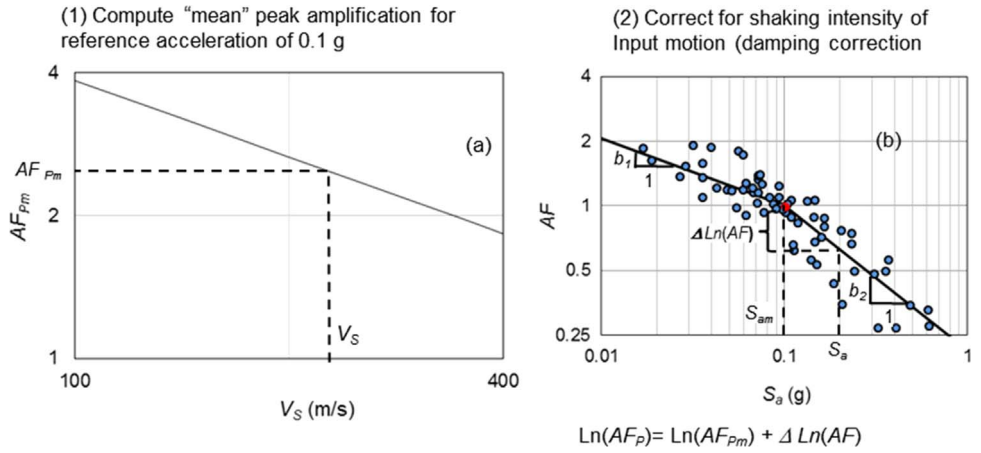

Fig. 9. Schematic illustration to compute peak amplification factor.

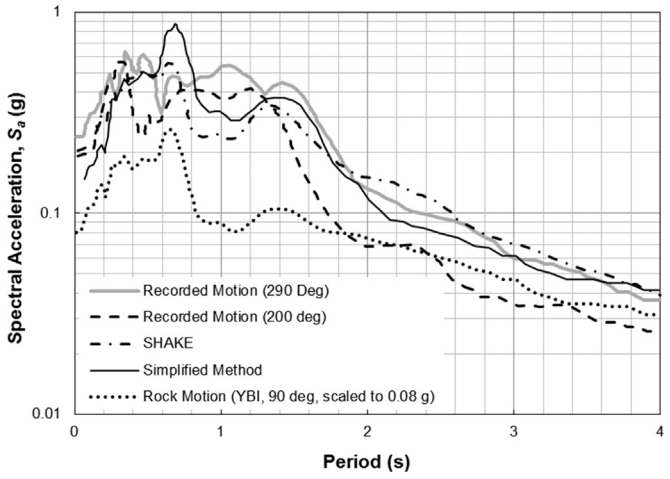

Fig. 10. Verification of proposed simplified method for case of 2-Story Oakland Building shaken by Loma Prieta (1989) earthquake.

Table 4
Soil Profile at Oakland 2-Story Building Site [23].

Layer No.	Soil Type	Depth (m)		Thickness (m)	Average V_S (m/s)
		From	To		
1	Sand	0.0	1.2	1.2	140
2	Sandy Clay	1.2	14.6	13.4	168
3	Sandy Gravel	14.6	18.9	4.3	305
4	Sandy Clay	18.9	27.8	8.9	230
5	Gravelly Sand	27.8	32.3	4.5	381
6	Old Bay Clay	32.3	86	53.7	338
7	Alluvium	86	152.4	66.4	695
8	Bedrock	152.4	–	–	1070

two components of surface motions recorded for this site (200 deg and 290 deg) are plotted in Fig. 10. The subsurface layers and average V_S values are presented in Table 4. Note a sharp contrast in V_S profile between layers 4 and 5. For the purpose of applying the simplified procedure we created an idealized soil profile consisting of two layers:

- Upper softer layer from 0 to 27.8 m with average V_S=197 m/s,
- Lower stiffer layer from 27.8 to 86 m with average V_S=340 m/s.

The proposed simplified procedure was implemented twice in the following order: Analysis I: the rock outcrop motion was applied on top of layer No.7 (V_S=695 m/s) and propagated through sublayers 5 and 6 (assuming average V_S=340 m/s), Analysis II: the calculated response on top of layer 5 from Analysis I was applied as input motion to base of layer No. 4 and propagated through sublayers 1 through 4 (assuming average V_S=197 m/s) to calculate response at the ground surface. Considering majority of underlying soils consist of clay or sandy clay, we used the generic clay model.

The detailed calculation steps and intermediate parameters computed in simplified procedure are summarized in Table 5. The calculated response using simplified procedure along with the calculated response using SHAKE by Sun et al. [25] are plotted in Fig. 10. The surface response spectra estimated based on simplified procedure agrees well with SHAKE results and both methods generally provide a reasonable estimation of surface response represented by two recorded surface motions. The simplified procedure underestimates the response at very short period which can be attributed to over-simplification of soil profile. Also note that the simplified procedure provides a better estimate of amplification than SHAKE at proximity of 1.0 s. In general, the discrepancy between simplified procedure and recorded motions can be a result of the selection of input rock motions, limitations of the one-dimensional model, limitation of equivalent-linear method, idealization of soil profile, and unaccounted soil-structure interaction effects.

5. Conclusions

1. Single proxy approach is widely used to estimate the effect of near surface soils on seismic demand. Numerous studies have investigated merits of proposed proxies including shear wave velocity (V_S) averaged in top 30 m and site period with some contradicting results. This has left the debate over selecting the best "site proxy" unsettled.
2. We used a methodology that allowed isolating and tracking the impact of components that drive site response including V_S, site period, and shaking intensity. We performed a parametric study on 19 hypothetical shallow profiles each shaken by 74 records from 27 earthquakes using one-dimensional equivalent-linear method. The results were analyzed to identify trends.
3. The effect of V_S on site response was quantified by tracking maximum amplification factor across the period range, averaged from 74 records for each soil profile. Soil type-specific relationships were developed for amplification as a function of V_S.
4. Nonlinear soil behavior impacts site response through two mechanisms: "damping increase" which de-amplifies the motion; and "migration of site period" which may amplify or de-amplify the motion depending on the direction of site period shift with respect to period of interest. Amplification factor at a given period increases with shaking intensity when site period migrates towards period of interest.

Table 5
Calculation Steps for Oakland 2-story Building following Simplified Procedure.

Calculation Steps	Analysis No. Layers included in soil column Base level	I #5, 6 to compute motion at top of layer #5 Top of layer #7	II #4, 3, 2, 1 to compute motion at top of layer #1 Top of layer #5
Step 1: Determine Site Parameters	V_S (m/s)	341	197
	H(m)	58	28
	T_N (s)	0.68	0.56
Step 2: Determine Motion Parameters	PGA (g)	0.08	0.08
	S_a 0.6 s (g	0.24	0.35
	S_a 1.0 s (g)	0.09	0.16
	$S_a{}^F$ (g)	0.25	0.34
Step 3: Determine Strain Compatible Site Period	$V_S{}^*/V_S$	0.91	0.86
	$T_N{}^*$ (s)	0.76	0.62
	$V_{Sm}{}^*/V_S$	0.96	0.95
	$T_{Nm}{}^*$ (s)	0.71	0.59
Step 4: Determine Amplification factor at periods of 0.1 s, 0.6 s, 1.0 s	Mean $AF_{0.1}$	1.0	1.5
	Δ Ln $(AF_{0.1})$	0.01	0.04
	$AF_{0.1}$	1.01	1.56
	Mean $AF_{0.6}$	1.6	2.1
	Δ Ln $(AF_{0.6})$	0.1	0.13
	$AF_{0.6}$	1.45	1.85
b values for damping correction:	Mean $AF_{1.0}$	1.7	2.1
	Δ Ln $(AF_{1.0})$	0	0
	$AF_{1.0}$	1.7	2.1
	$AF_{3.0}$	1.2	1.1
0.1 s			
b_1 = −0.05 for Analysis No.1			
b_1 = −0.17 for Analysis No.2			
0.6 s			
b_2 = −0.11 for Analysis No.1			
b_2 = −0.10 for Analysis No.2			
1.0 s			
Damping correction not required			
because $T_N{}^*$ < 1.0 s			
Step 5: Compute Peak Amplification Factor	AF_{Pm}	1.94	2.61
	Δ Ln (AF_P)	0.02	0.06
	AF_P	1.90	2.45
b values for damping correction:			
b_1 = −0.02 for Analysis No.1			
b_1 = −0.05 for Analysis No. 2			

5. Depth-specific and depth-independent models were analyzed for amplification versus shaking intensity. We found the residual standard deviation of amplification factor, $\sigma_{Ln(AF)}$, using a depth-independent model are up to three times larger than $\sigma_{Ln(AF)}$ based on depth-specific model. Using a depth-independent model generates additional uncertainty which is epistemic in nature, that is, can be removed provided that suitable models are used.
6. $\sigma_{Ln(AF)}$, ranges from 0.06 to 0.34 at short and mid periods, 0.03–0.13 at long period, and 0.04–0.12 for peak amplification factor. These results generally match the $\sigma_{Ln(AF)}$ range of less than 0.3 reported by Bazzurro and Cornell [4] based on two soil profiles.
7. Plots of amplification versus strain compatible site period provide a holistic prospective of how V_S, strain compatible site period, and damping contribute in site response. These three components contain mutually exclusive predictive information regarding site response. Trend lines were presented for different V_S values to estimate amplification factor as a function of strain compatible site period at different periods. A method was presented to correct amplification factor for damping effects.
8. A simplified procedure is proposed to address the need in current state of practice for an intermediate site response solution between the rigorous numerical solutions on one end and the generic site factors on the other end. We applied the proposed procedure to a building site shaken by Loma Prieta (1989) earthquake. The predicted amplification factors match reasonably well with recorded motion at the surface and also one-dimensional site response analysis by SHAKE.

References

[1] Abrahamson NA, Silva WJ. Empirical response spectral attenuation relations for shallow crustal earthquakes. Seismol Res Lett, 1997 V 1997;68(1):94–127.
[2] Abrahamson NA, Silva WJ. Summary of the Abrahamson & Silva NGA ground-motion relations. Earthq Spectra 2008;24(1):67–97.
[3] Baturay MB, Stewart JP. Uncertainty and bias in ground motion estimates from ground response analyses. Bull Seismol Soc Am 2003;94:2090–209.
[4] Bazzurro, P, Cornell, CA. Ground motion amplification in nonlinear soil sites with uncertain properties, Bull. Seismol. Soc. Am. 94; 2004. 2090–209.
[5] Borcherdt RD. Estimates of site-dependent response spectra for design (methodology and justification). Earthq Spectra 1994;10:617–53.
[6] Borcherdt RD. Empirical evidence for acceleration-dependent amplification factors. Bull Seismol Soc Am 2002;95:373–4.
[7] Boore DM, Atkinson GM. Ground-motion prediction equations for the average horizontal component of PGA, PGV, and 5%-Damped PSA at Spectral Periods between 0.01 s and 10.0 s. Earthq Spectra 2008;24(1):99–138.
[8] Campbell KW, Bozorgnia Y. NGA ground motion model for the geometric mean horizontal component of PGA, PGV, PGD and 5% damped linear elastic response spectra for periods ranging from 0.01 to 10 s. Earthq Spectra 2008;24(1):139–71.
[9] Castellaro, S, 2011. The VFZ matrix: Simplified seismic soil classification from a different perspective, in Fourth IASPEI/IAEE International Symposium: Effects of Surface Geology on Seismic Motion, University of California, Santa Barbara, 23-26 August 2011, http://esg4.eri.ucsb.edu/sites/default/files/Castellaro%20ESG4%20Vs30.pdf (last Accessed September 2014).
[10] Castellaro S, Mulargia F, Rossi PL. V_{S30}: Proxy Seism Amplif? Seismol Res Lett 2008;79(4):540–3.
[11] Bolisetti C, Whittaker AS, Masonb HB, Almufti I, Willford M. Equivalent linear and nonlinear site response analysis for design and risk assessment of safety-related nuclear structures. Nucl Eng Des 2014;v275:107–21.
[12] Chiou BS-J, Youngs RR. An NGA model for the average of horizontal component of peak ground motion and response spectra. Earthq Spectra 2008;24(1):173–216.
[13] Choi Y, Stewart JP. Nonlinear site amplification as function of 30 m shear wave velocity. Earthq Spectra 2005;21:1–30.
[14] Darendeli M. Development of a new family of normalized modulus reduction and material damping curves [Ph.D. Thesis]. Austin, Texas: Univ. of Texas; 1991.
[15] Kaklamanos James, Baise Laurie G, Thompson Eric M, Dorfmann Luis. Comparison of 1D linear, equivalent-linear, and nonlinear site response models at six KiK-net validation sites. Journal of Soil Dynamics and Earthquake ENgineering 2015;69:207–19.
[16] Joyner WB, Boore DM. Recent developments in earthquake ground motion estimation, In: Proceedings of the 6th International Conference on Seismic Zonation, Earthquake Engineering Research Institute, Oakland, CA; 2000.
[17] National Earthquake Hazard Reduction Program [NEHRP]. Recommended Provisions for Seismic Regulations for New Buildings and Other Structures , FEMA P-750/2009
[18] Ordonez G. SHAKE2000, A computer program for the 1-D analysis of geotechnical earthquake engineering problems; 2004.
[19] McVerry, G.H. ite-effect terms as continuous functions of site period and Vs30. 9Th Pacific Conference on Earthquake Engineering, Auckland, New Zealand; 2011.
[20] Rodriguez-Markez A, Bray JD, Abrahamson NA. An empirical geotechnical seismic site response procedure. Earthq Spectra 2001;17:65–87.
[21] Schnabel PB. Effects of Local Geology and Distance from Source on Earthquake Ground Motions [PhD thesis]. Berkley, California: University of California; 1973.
[22] Seed HB, Idriss IM. Soil moduli and damping factors for dynamic response analyses [Report no. EERC70-10]Earthquake Engineering Research Center. Berkeley, California: University of California; 1970.
[23] Stewart JP, Liu AH, Choi Y. Amplification factors for spectral acceleration in

tectonically active regions. Bull Seismol Soc Am 2003;93:332–52.
[24] Sun JI, Golesorkhi R, Seed HB. Dynamic moduli and damping ratios for cohesive soils [Report No. EERC 88-15]Earthquake Engineering Research Center. Berkeley, California: Univ. of California; 1988.
[25] Sun JI, Bray JD, Chang SW, Mejia LH.Damage Patterns/Response of Deep Stiff Clay in Oakland, : In: Proceedings of the Third International Conference on Case Histories In Geotechnical Engineering, St. Louis, Missouri; 1993.
[26] Steidl JH. Site response in southern California for probabilistic seismic hazard analysis. Bull Seismol Soc Am 2000;90:S149–S169.
[27] Uniform Building Code, 1997. Structural engineering design provisions, International Conference of Building Officials.
[28] Walling M, Silva W, Abrahamson N. Nonlinear site amplification factors for constraining the NGA models. Earthq Spectra 2008;24:243–55.
[29] Zhao JX, Irikura K, Zhang J, Fukushima Y, Somerville PG, Asano A, Ohno Y, Oouchi T, Takahashi T, Ogawa H. An empirical site classification method for strong motion stations in Japan using H/V response spectrum ratio. Bull Seismol Soc Am 2006;96:914–25.
[30] Zhao JX. Comparison between VS30 and site period as site parameters in ground-motion prediction equations for response spectra, In: Proceedings of the 4th IASPEI / IAEE International Symposium: Effects of Surface Geology on Seismic Motion August 23–26, 2011, University of California Santa Barbara; 2011.